



NOTE

Microfabrication of scaffold-free tissue strands for three-dimensional tissue engineering

To cite this article: Adil Akkouch *et al* 2015 *Biofabrication* 7 031002

View the [article online](#) for updates and enhancements.

You may also like

- [Current biofabrication methods for vascular tissue engineering and an introduction to biological textiles](#)
Fabien Kawecki and Nicolas L'Heureux
- [Scaffold-based and scaffold-free cardiac constructs for drug testing](#)
Kenichi Arai, Takahiro Kitsuka and Koichi Nakayama
- [Scaffold-free approaches for the fabrication of engineered articular cartilage tissue](#)
Kang Sun, Chao Tao and Dong-An Wang

Biofabrication



NOTE

Microfabrication of scaffold-free tissue strands for three-dimensional tissue engineering

RECEIVED
26 June 2015

REVISED
16 August 2015

ACCEPTED FOR PUBLICATION
21 August 2015

PUBLISHED
16 September 2015

Adil Akkouch¹, Yin Yu¹ and Ibrahim T Ozbolat^{1,2,3,4}

¹ Biomanufacturing Laboratory, Center for Computer-Aided Design, The University of Iowa, IA City, USA

² Department of Mechanical Engineering and Industrial Engineering, The University of Iowa, IA City, USA

³ Engineering Science and Mechanics Department, The Pennsylvania State University, State College, USA

⁴ The Huck Institute of the Life Sciences, The Pennsylvania State University, State College, USA

E-mail: ibrahim-ozbolat@uiowa.edu

Keywords: tissue strands, micro-fabrication, cell aggregation, mini-tissue building blocks

Abstract

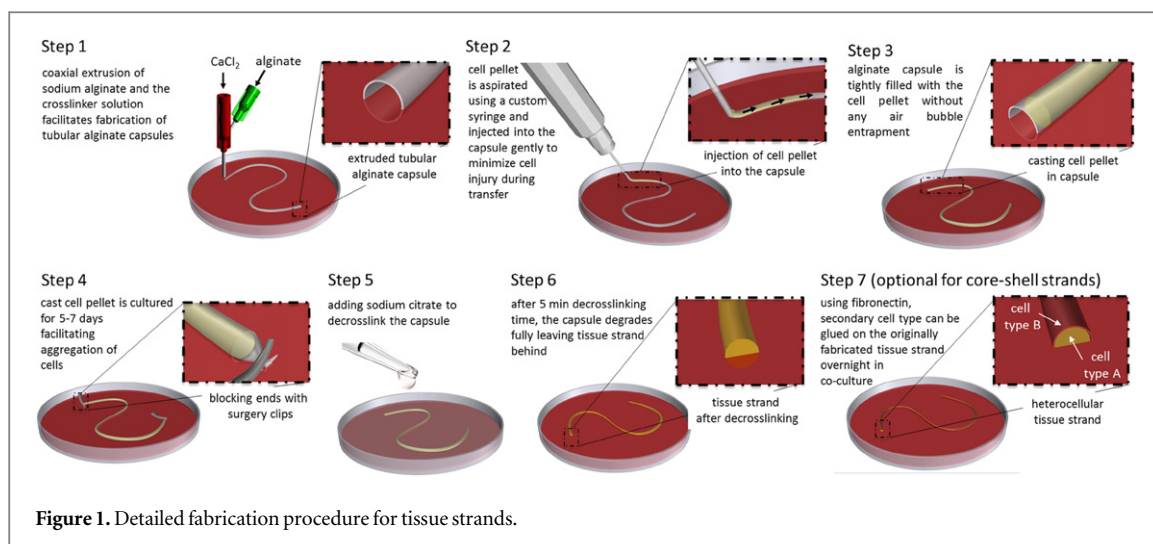
In this note, we report a practical and efficient method based on a coaxial extrusion and microinjection technique for biofabrication of scaffold-free tissue strands. Tissue strands were obtained using tubular alginate conduits as mini-capsules with well-defined permeability and mechanical properties, where their removal by ionic decrosslinking allowed the formation of scaffold-free cell aggregates in the form of cylindrical strands with well-defined morphology and geometry. Rat dermal fibroblasts and mouse insulinoma beta TC3 cells were used to fabricate both single-cellular and heterocellular tissue strands with high cell viability, self-assembling capability and the ability to express cell-specific functional markers. By taking advantage of tissue self-assembly, we succeeded in guiding the fusion of tissue strands to fabricate larger tissue patches. The presented approach enables fabrication of cell aggregates with controlled dimensions allowing highly long strands, which can be used for various applications, including fabrication of scale-up complex tissues and of tissue models for drug screening and cancer studies.

1. Introduction

Mini-tissue fabrication has shown great promise in creating complex tissues and organs for medical use [1]. The precise assembly and spatial deposition of cell aggregates leads to the fabrication of three-dimensional (3D) anatomical structures like organs [2]. Typically, cells are conditioned to self-aggregate to form scaffold-free mini-tissue blocks and then assembled into multicellular constructs to fabricate complex tissue and organ modules [3, 4]. Tissue spheroids, which are spherical-shaped cell aggregates, have been shown their potential as building blocks for scale-up tissue fabrication [5]. Tissue spheroids can easily mimic architectural and functional characteristics of their native tissue; when spheroids are in contact with each other, they fuse and coalesce into a cohesive tissues such as blood vessels [6], skin [7], nerves [8] and dental pulp [9]. Several methods are used to produce tissue spheroids, including hanging drop, micro-molding, magnetic levitation, spinning flask, non-adherent substrate, and cell trapping using

microfluidic devices [10, 11]; however, the formed aggregates may have irregular geometry and size, weak reproducibility, and difficulties during harvesting and scale-up tissue fabrication processes. In addition, lack of contact between cell aggregates can affect the precision of spatial placement and fusion, and gap formation between spheroids may compromise the self-assembling and maturation process, leading to the failure of tissue regeneration. Indeed, technologies should be developed to fabricate cell aggregates with well-controlled dimensions in a scalable form to assure practicality for scale-up fabrication of tissues.

In this note, we report a novel method, which enables scale-up fabrication of mini-tissue building blocks in strand form called 'tissue strands.' Tissue strands made of different cell types were fabricated within semi-permeable tubular alginate capsules that were directly extruded using a coaxial nozzle apparatus. A cell viability test revealed minimal cell damage upon fabrication, and tissue strands demonstrated self-assembling capability. Immunofluorescence staining showed overall tissue-specific markers'



expression on matured tissue models. Hybrid fabrication of heterocellular tissue strands was also presented, showing their potential for fabrication of a pancreatic tissue model. Our study presents a practical method for cell aggregation in strand form with controlled dimensions, which might serve as miniaturized functional tissue blocks for scale-up tissue fabrication, drug screening, tissue printing and creation of tumor models for cancer studies.

2. Materials and methods

2.1. Fabrication of microfluidic tubular alginate capsules

In this work, we used coaxially extruded alginate capsules to cast cell pellet for tissue strand fabrication. The coaxial extrusion method, as detailed in our earlier work, facilitated generation of mini-capsules in uniform size and highly round shape made of non-toxic, low-cost and flexible alginate [12, 13]. Briefly, a sodium alginate 4% (w/v) solution in deionized water (dH₂O) (Sigma Aldrich, USA) was used in this study as biomaterial for tubular alginate capsule fabrication, and a 4% (w/v) solution of calcium chloride (CaCl₂) (Sigma Aldrich, USA) in (dH₂O) was used as a crosslinking agent. The fabrication system consisted of a homemade coaxial nozzle unit connected to a pneumatic air dispenser (EFD[®] Nordson, USA) and a mechanical pump (New Era Pump System Inc., USA) for alginate and CaCl₂ extrusion, respectively. The coaxial nozzle assembly was composed of a 22G inner nozzle (0.71 mm and 0.41 mm for outer and inner diameter, respectively) and a 14G outer nozzle (2.11 mm and 1.69 mm for outer and inner diameter, respectively). The alginate-dispensing pressure was set at 82.7 kPa, while the CaCl₂ dispensing rate was set at 16 ml min⁻¹. Pre-crosslinked alginate tubular capsules were extruded into a CaCl₂ pool and left overnight for complete crosslinking.

2.2. Cell preparation

Primary rat dermal fibroblasts (RDFs) (ATCC, USA) were cultured in α -minimum essential medium (α -MEM) supplemented with 10% fetal bovine serum (FBS), 100 U mL⁻¹ penicillin G, 25 μ g mL⁻¹ streptomycin and 0.5 μ g mL⁻¹ fungizone (all from Life Technologies, USA). Mouse insulinoma beta TC3 (β TC-3) cells, a kind gift from Dr Nicolas Zavazava's laboratory (The University of Iowa, USA), were cultured in Dulbecco's Modified Eagle's Medium supplemented with 10% FBS, 1 mM sodium pyruvate, 5 mM Glutamax, 100 U mL⁻¹ penicillin G, 25 μ g mL⁻¹ streptomycin, 0.5 μ g mL⁻¹ fungizone and 10 mM MEM non-essential amino acids (all from Life Technologies, USA). Cells were maintained at 37 °C with 5% CO₂ in an air-humidified atmosphere. Cell culture medium was changed every 2–3 d. Subconfluent cultures were detached from the flasks using a 0.25% trypsin-0.1% EDTA solution (Life Technologies, USA), washed twice, and split to maintain cell growth. Cells in passages 4–7 were used for each experiment.

2.3. Biofabrication of tissue strands

The fabrication procedure is demonstrated in figure 1. Briefly, cells (RDF or β TC-3) were harvested using 0.25% trypsin-0.1% EDTA solution and centrifuged at 3500 rpm. The resulting pellet was incubated at 37 °C with 5% CO₂ overnight in α -MEM media supplemented with 10% FBS and 15 mM HEPES, in order to have sufficient coherency and mechanical integrity during further processing. Cell pellet was then injected into tubular alginate capsules by a custom syringe unit (Hamilton Company, USA), and ends were tied using vessel clips (World Precision Instrument, USA). The injected pellet was incubated for 5 d, and then alginate was dissolved in a 1% sodium citrate solution in dH₂O (Sigma Aldrich, USA) for 5 min, leaving pure cellular tissue strands. The morphology of tissue strands was monitored using an inverted microscope (Leica

Microsystems Inc., USA) equipped with a digital camera, and dimension measurements were conducted using NIH Image J software (National Institutes of Health, USA).

2.4. Cell viability and proliferation studies

Cell viability was tested after 3, 5 and 7 d of culture with the Trypan Blue standard method [14]. Tissue strands 5 mm in length were washed and incubated with a 0.25% trypsin-0.1% EDTA solution for 3 min at 37 °C. Dispersed cells were collected and mixed with Trypan Blue solution (0.4%) at 1:1 ratio (v/v) (Sigma Aldrich, USA). The suspension was loaded into a hemocytometer and visualized under an inverted microscope (Leica Microsystems Inc., USA); dead cells take up the blue dye (Trypan Blue positive). The cell viability was calculated by dividing the number of live cells by the total number of cells and multiplying by 100. The proliferation of injected cells was quantified by means of MTT (3-(4, 5-dimethylthiazol-2-yl)-2, 5-diphenyltetrazolium-bromide) assay (Life Technologies, USA), which directly measures the cellular metabolic activity through the biodegradation of tetrazolium salt by viable and active cells. Briefly, tissue strands 5 mm in length were cultured in the presence of a 1% (v/v) MTT solution (5 mg mL^{-1}) for 4 h at 37 °C and 5% CO₂. Following the culture period, the formazan precipitate was extracted using isopropanol (Sigma Aldrich, USA), and 200 μL (in triplicate) of the supernatant was transferred from each well to a 96-well flat-bottom plate, and the absorbance was determined at 550 nm using a microplate reader (Bio-Tek PowerWave X, USA).

2.5. Scanning electron microscopy imaging

Field emission SEM (Hitachi S-4800, Japan) was used to investigate the ultra-morphology of fibroblast tissue strands. After dissolving alginate capsules, tissue strands were fixed in 4% paraformaldehyde (Sigma Aldrich, USA) for one hour and then dehydrated in graded ethanol solutions (50%–100%). Afterwards, samples were chemically dried with hexamethyldisilazane (Sigma Aldrich, USA), sputter-coated (K550 Emitech Sputter Coater) (Quorum Technologies Limited, UK) and then observed at an accelerating voltage of 1.5 kV.

2.6. Fabrication of hybrid tissue strands

Matured fibroblast tissue strands were co-cultured with $\beta\text{TC-3}$ cells in suspension. Briefly, fibroblast tissue strands were released from alginate minicapsules by adding 1% sodium citrate (Sigma Aldrich, USA) solution in dH₂O for 5 min followed by three washings with warmed culture media and incubated in a humidified incubator at 37 °C overnight. Fibroblast mini-tissues were coated with fibronectin solution ($10 \mu\text{g mL}^{-1}$) (Sigma Aldrich, USA), and then $\beta\text{TC-3}$ cells in dense suspension were added to fibroblast

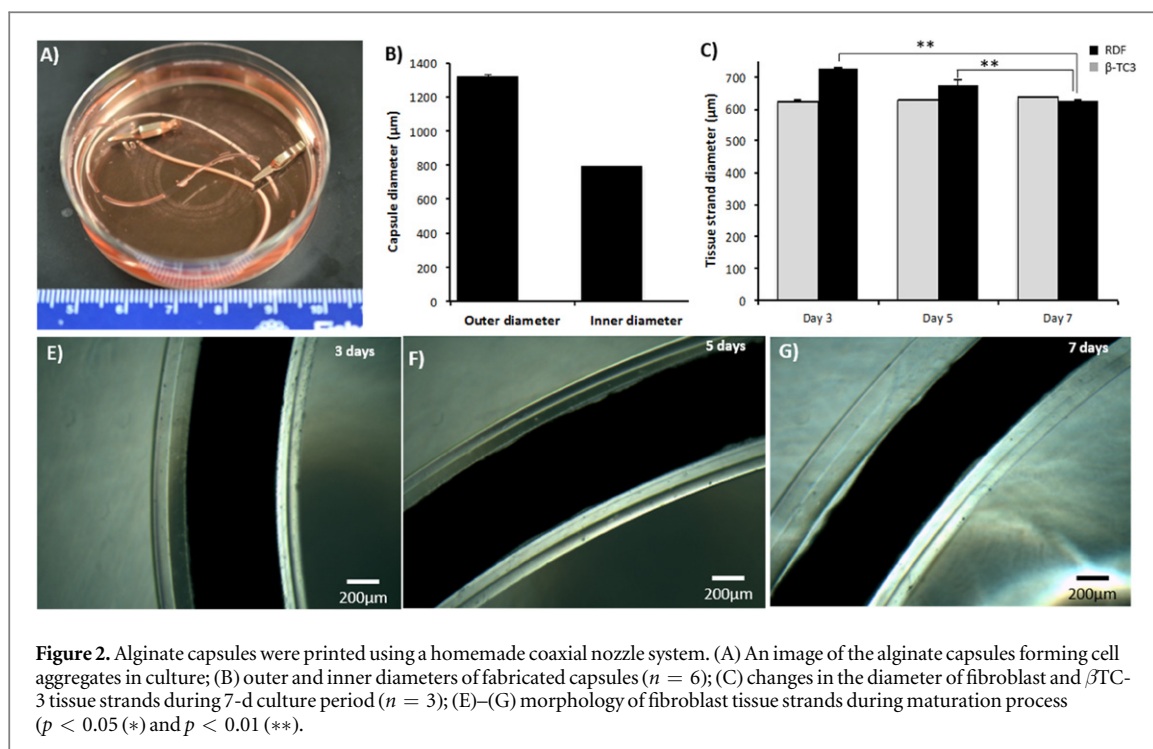
mini-tissues and cultured at 37 °C with 5% CO₂ in an air-humidified atmosphere for 24 h to allow $\beta\text{TC-3}$ cell adhesion and fusion on the fibroblasts core layer as shown in step 7 in figure 1.

2.7. Immunofluorescence imaging

To evaluate tissue-specific protein expression, immunofluorescence staining was used for fibroblasts and $\beta\text{TC-3}$ cell specific markers. After fixation in 4% paraformaldehyde (Sigma Aldrich, USA), tissue strands were permeabilized for 15 min using 0.3% Triton X-100 and incubated 1 h with 0.3% of cold water fish skin gelatin (Sigma Aldrich, USA) in PBS to block unspecific staining. Fibroblast tissue strands were incubated overnight with E-Cadherin primary antibody (Dako, Denmark) then further washed with PBS and incubated with secondary antibody, a goat anti-mouse Alexa 488 (Life Technologies, USA), for 60 min at room temperature, followed by incubation with Phalloidin Alexa 568 (Life Technologies, USA) for 30 min. Tissue strands made of $\beta\text{TC-3}$ cells were incubated overnight with Insulin primary antibody (abcam, USA) and C-peptide primary antibody (Cell Signaling, USA) and then washed with PBS and incubated with secondary antibodies, a Goat anti-guinea pig Alexa 488 and a goat anti-rabbit Alexa 568 (Life Technologies, USA), for 60 min at room temperature. However, heterocellular tissue strands were incubated overnight with insulin primary antibody (abcam, USA), washed with PBS, and then incubated with secondary antibody, a goat anti-guinea pig Alexa 488 (Life Technologies, USA), for 60 min at room temperature, followed by incubation with Phalloidin Alexa 568 (Life Technologies, USA) for 30 min. Stained samples were mounted using Vectashield mounting medium with DAPI (Vector Laboratories, USA) and examined with a laser-scanning confocal fluorescence microscopy Carl Zeiss—LSM 710 (Carl Zeiss, Germany).

2.8. Self-assembly of tissue strands

Self-assembly is a characteristic property of cell aggregates, which granted them the capability to form larger tissue upon contact. Fusion experiments were carried out to test the potential of tissue strands to self-assemble into larger tissue. Briefly, multiple individual constructs were placed onto a 150 mm petri dish close to each other with contact and confined by polycaprolactone (Scientific Polymer Products, Inc., USA) mold. A minimum amount of culture media was supplemented into the cultures, ensuring cell survival without losing their contact. Calcein AM (Life Technologies, USA) was used for cell staining, and fluorescence microscopic images (Leica Microsystems Inc., USA) were taken at different time points to monitor the fusion process with minimal disturbance.



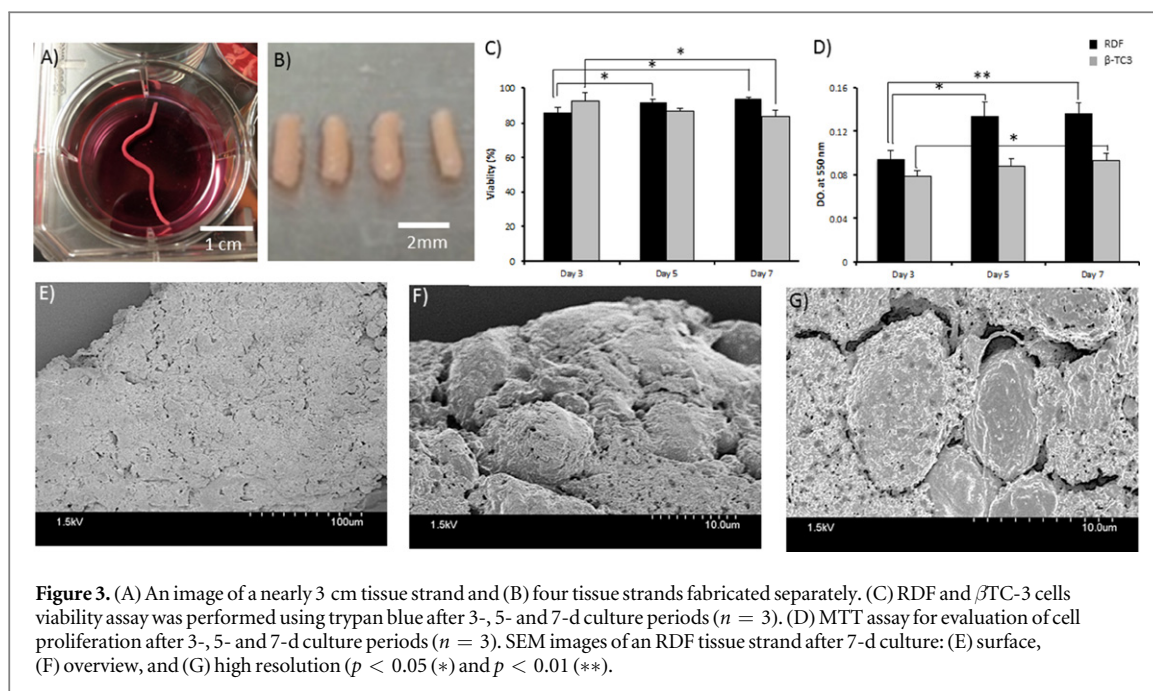
2.9. Statistical analysis

Data were presented as mean \pm standard deviation of three independent experiments. Statistical comparison between two groups was determined using student's t-test using MS Excel. Differences were considered significant at $p < 0.05$ (*) and $p < 0.01$ (**).

3. Results and discussions

Tubular capsules were successfully extruded with uniform morphology, and cells were micro-injected in them, as presented in figure 2(A). The average lumen diameter and outer diameter of the fabricated alginate capsules were $791.06 \pm 4.03 \mu\text{m}$ and $1319.92 \pm 9.16 \mu\text{m}$, respectively ($n = 6$) (see figure 2(B)). The process variation was highly small while a capsule was extruded as a single piece and cut into multiple pieces after extrusion. By controlling fabrication parameters, different sizes of capsules could be fabricated as detailed in our earlier work [13], where the smallest capsule diameter and wall thickness were reported as $617 \mu\text{m}$ and $175 \mu\text{m}$, respectively. The printed capsules were malleable with sufficient flexibility and permeability to allow oxygen and media exchange in culture [12]. By controlling printing parameters, various sizes with different wall thickness of capsules could be produced upon demand for further tissue strand fabrication. While non-modified alginate surface is inert to cell adhesion, mini-capsules allowed aggregation of cells quickly in culture, and the capsules were highly flexible, allowing easy handling of the strands.

Cell pellet was successfully transferred into alginate mini-capsules over 10 cm long, with minimum injury of cells. Cellular material was cast into the alginate capsules with close contact to the inner wall. The proposed approach enables micro-injection of cell pellet in any volume and there is no limit with the length of the tissue strands. About 13 million fibroblasts were used per 1 mm of tissue strands but this number depends on the lumen diameter of the capsules as well as average cell diameter. Cultured cells formed compact tissue strands with good integrity and structural strength both before and after decrosslinking the alginate capsules after 7 d of *in vitro* incubation. The diameter of formed β TC-3 tissue strands remained stable during the 7-d culture period (see figure 2(C)) (day 3: 625.05 ± 2.28 , day 5: 627.45 ± 0.81 , and day 7: 634 ± 0.99 ($n = 3$)), resulting in mechanically and structurally weak constructs; however, fibroblast tissue strands started to diminish in radial axis due to contraction, during which visible gaps were observed between the outer surface of tissue strands and the inner wall of alginate capsules (see figures 2(E)–(G)). The dimension of fibroblast tissue strands changed over time: 724.60 ± 6.38 , 682.59 ± 13.62 and $633.53 \pm 3.34 \mu\text{m}$ ($n = 3$) in diameter after 3, 5 and 7 d culture period, respectively. The shrinkage of maturing tissue strands is mainly due to the normal contraction of healthy cultures of stromal cells in a 3D environment and the contractile potential of fibroblasts and the high cell-to-cell interaction in 3D culture system [15]. The weak nature of β TC-3 tissue strands can be attributed to the limited ability of



β TC-3 to deposit extracellular matrix (ECM) components of connective tissues.

After a 7-d culture period, alginate capsules were decrosslinked and cut into smaller pieces. Figure 3(A) shows highly long (nearly 3 cm) tissue strand that was malleable, mechanically and structurally integrated and intact enough to enable ease of handling and figure 3(B) demonstrates shorter tissue strands fabricated in different capsules. Cell viability was maintained upon fabrication as well as during culture. The average viability of RDF tissue strands on day 3 post-fabrication was $85.87\% \pm 2.85\%$, gradually increased to $91.73\% \pm 1.51\%$ on day 5, and finally reached $93.54\% \pm 0.98\%$ on day 7 ($n = 3$) (see figure 3(C)). β TC-3 strands presented high cell viability after 3 d culture $92.83\% \pm 4.29\%$ and decreased to $86.68\% \pm 1.50\%$ and $83.57\% \pm 3.28\%$ after 5 and 7 d, respectively ($n = 3$) (see figure 3(C)). The authors speculate that this might be due to the weak capability of beta cells to recover from injury caused by shear stress during the injection step, as well as hypoxia-induced cell death in the core section of the strand (see figure 4(D) with weak DAPI signal) when the diameter exceeds diffusion limits depending on the matrix density and permeability, which can be alleviated using capsules with smaller diameter. Although cell viability was assessed for a week, β TC-3 viability may decrease further in the longer term due to its trend, which can be alleviated by reducing the diameter of β TC-3 strands.

Growth measurement by means of MTT assay confirmed the viability analysis (see figure 3(D)). RDFs showed a high growth rate when cultured within alginate mini-capsules. This trend was maintained at 3-, 5- and 7-d culture periods. The growth level of β TC-3 cells within alginate mini-capsules was reduced

compared to that of fibroblasts. Indeed, cultured fibroblasts within alginate mini-capsules showed a high number of viable and proliferative cells. This high proliferative rate of fibroblasts was maintained at days 3 and 5, but stabilized at day 7. At day 7, tissue strands presented high integrity, maturity and ECM deposition, as shown in SEM images. Figures 3(E)–(G) show the ultrastructure of RDF tissue strands after 7 d of culture. Injected fibroblasts in high density formed compact tissue strands with tight cell-to-cell adhesion and abundant ECM deposition. Confluent fibroblast cell cultures are known to secrete ECM and to initiate fibrillogenesis, leading to the accumulation of a thick matrix composed of fibronectin and collagen type I [16, 17]. The synthesized fibrils network promoted further focal-adhesion assembly and increased contractility of the fabricated fibroblast tissue strands. Furthermore, it has been shown that the expression of transforming growth factor, beta 3 mRNA, a cytokine related to wound healing, increases in 3D fibroblast aggregates when compared to that in a 2D culture system [18]. Such conformation allows the adhesion and the integration of β TC-3 cells around fibroblast tissue strands. In addition, the fibroblast compartment played a key role as a feeder core for the β TC-3 cell layer and supported tissue strands mechanically and structurally for easy handling.

Phalloidin immunostaining of fibroblast tissue strands showed a parallel orientation of the cells to the stretching direction (see figures 4(A) and (B)). Fibroblasts' orientation in tissue strands resulted from increased cell-to-cell adhesion as confirmed by high expression of E-cadherin and radial shrinkage of the construct during maturation. Cultured β TC-3 in alginate capsules maintained high expression of insulin and C-peptide (a precursor for insulin) (see

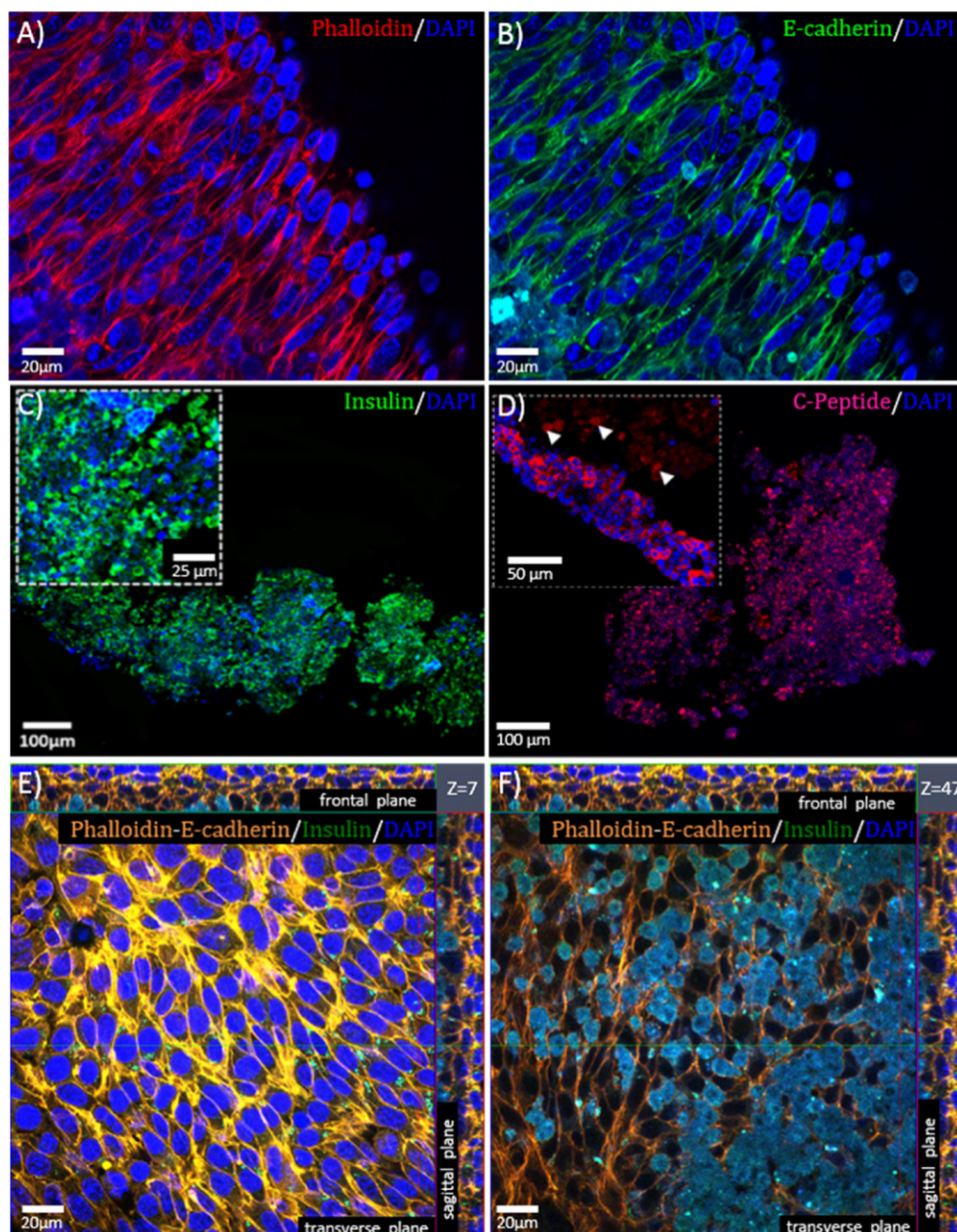


Figure 4. Confocal microscopy of specific tissue proteins related to RDF and β TC-3: (A) phalloidin (red) and (B) E-cadherin (green) staining was performed on RDF tissue strands; (C) insulin (green) and (D) C-peptide staining was performed on β TC-3 tissue strands. Triple staining was performed on heterocellular tissue strands using phalloidin/E-cadherin (merged: orange) and insulin (green) specific antibodies; cross-sections of the confocal-z-planes (E) representing the fibroblast core layer (z -plane = 7) and (F) represents the outer layer made by β TC-3 cell (z -plane = 47). Nuclei were stained non-specifically with DAPI (blue).

figures 4(C) and (D)). While structural integrity of β TC-3 strands was weak, disintegration was observed during sectioning process for histology study. To evaluate the expression of tissue-specific proteins in heterocellular tissue strands, two markers were used for immunofluorescence labeling with specific antibodies. As shown in figures 4(E) and (F), a substantial amount of superficial cells were positively stained with insulin (green) ($z = 47$) in whole tissue. However, the core region ($z = 7$) made by fibroblast was negatively stained with insulin. This indicates that β -cells were integrated with the fibroblast core, generated a thin layer, and maintained insulin expression capability.

Tissue strands stained with Calcein AM (see figure 5(A)) underwent a fusion test. Self-assembly-driven fusion started as early as 24 h post-fabrication during incubation (see figure 5(B)). At day 7, tissue strands were almost completely fused into a large single tissue patch due to interfacial tension, with contracted morphology, and no visible gap between strands (see figure 5(C)). In addition, tissue strands not only successfully fused to each other, but also integrated with β -cells, underwent remodeling and maturation in a prolonged culture period, and presented themselves as a seamless integrated pancreatic tissue model (data not shown here).

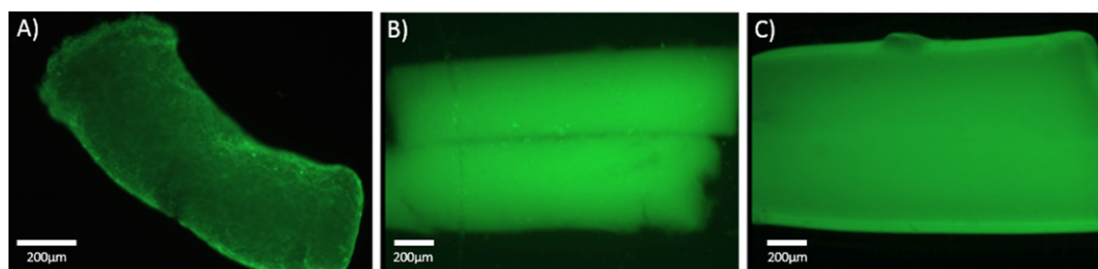


Figure 5. Fusion of tissue strands. (A) Tissue strands were stained with Calcein AM (green) and placed in contact with each other after releasing them from capsules post 5-d incubation. (B) Fusion started as early as 24 h, and (C) complete fusion was achieved in 7 d in culture.

4. Conclusion

This note presents a new method for practical fabrication of scaffold-free tissue strands using coaxially extruded alginate mini-capsules as a reservoir for cell aggregation in strand form. Dermal fibroblasts and β TC-3 cells are used to provide an example of the effectiveness of this method. Heterocellular pancreatic mini-tissue building blocks were also fabricated, demonstrating the flexibility of developing complex tissue models. Tissue strands exhibited high viability and cylindricity, negligible contractibility in the longitudinal axis, and rapid fusion capability, and they expressed cell-specific functional markers. The tissue strands presented in this work may have applications ranging from scale-up tissue printing and fabrication to development of tissue models for drug screening and cancer studies. For future work, we will directly extrude and print fabricated tissue strands in solid state without the need for a liquid delivering medium.

Acknowledgments

This work was supported by the National Science Foundation (CMMI CAREER 1349716), grants from the Diabetes in Action Research and Education Foundation, and the Grow Iowa Values Funds. The authors acknowledge Dr Nicolas Zavazava at the University of Iowa for kindly providing β TC-3 cells.

References

- [1] Khademhosseini A, Langer R, Borenstein J and Vacanti J P 2006 Microscale technologies for tissue engineering and biology *Proc. Natl Acad. Sci. USA* **103** 2480–7
- [2] Ozbolat I T and Yin Y 2013 Bioprinting toward organ fabrication: challenges and future trends *IEEE Trans. Biomed. Eng.* **60** 691–9
- [3] Guven S, Chen P, Inci F, Tasoglu S, Erkmén B and Demirci U 2015 Multiscale assembly for tissue engineering and regenerative medicine *Trends Biotechnol.* **33** 269–79
- [4] Lin R Z, Chu W C, Chiang C C, Lai C H and Chang H Y 2008 Magnetic reconstruction of three-dimensional tissues from multicellular spheroids *Tissue Eng. C Methods* **14** 197–205
- [5] Leferink A, Schipper D, Arts E, Vrij E, Rivron N, Karperien M, Mittmann K, van Blitterswijk C, Moroni L and Truckenmüller R 2014 Engineered micro-objects as scaffolding elements in cellular building blocks for bottom-up tissue engineering approaches *Adv. Mater.* **26** 2592–9
- [6] Mattix B M, Olsen T R, Casco M, Reese L, Poole J T, Zhang J, Visconti R P, Simionescu A, Simionescu D T and Alexis F 2014 Janus magnetic cellular spheroids for vascular tissue engineering *Biomaterials* **35** 949–60
- [7] Hsu S H and Hsieh P S 2015 Self-assembled adult adipose-derived stem cell spheroids combined with biomaterials promote wound healing in a rat skin repair model *Wound Repair Regen.* **23** 57–64
- [8] Jeong G S, Chang J Y, Park J S, Lee S A, Park D, Woo J, An H, Lee C J and Lee S H 2015 Networked neural spheroid by neuro-bundle mimicking nervous system created by topology effect *Mol. Brain* **8** 17
- [9] Dissanayaka W L, Zhu L, Hargreaves K M, Jin L and Zhang C 2014 Scaffold-free prevascularized microtissue spheroids for pulp regeneration *J. Dent. Res.* **93** 1296–303
- [10] Ota H and Miki N 2013 Microtechnology-based three-dimensional spheroid formation *Front Biosci. (Elite Ed)* **5** 37–48
- [11] Lin R Z and Chang H Y 2008 Recent advances in three-dimensional multicellular spheroid culture for biomedical research *Biotechnol. J.* **3** 1172–84
- [12] Zhang Y, Yu Y, Akkouch A, Dababneh A, Dolati F and Ozbolat I T 2015 *In vitro* study of directly bioprinted perfusable vasculature conduits *Biomater. Sci.* **3** 134–43
- [13] Zhang Y, Yu Y, Chen H and Ozbolat I T 2013 Characterization of printable cellular micro-fluidic channels for tissue engineering *Biofabrication* **5** 024004
- [14] Louis K S and Siegel A C 2011 Cell viability analysis using trypan blue: manual and automated methods *Methods Mol. Biol.* **740** 7–12
- [15] Yuge A, Nasu K, Matsumoto H, Nishida M and Narahara H 2007 Collagen gel contractility is enhanced in human endometriotic stromal cells: a possible mechanism underlying the pathogenesis of endometriosis-associated fibrosis *Hum. Reprod.* **22** 938–44
- [16] Park H J, Rouabhia M, Lavertu D and Zhang Z 2015 Electrical stimulation modulates the expression of multiple wound healing genes in primary human dermal fibroblasts *Tissue Eng. A* **21** 13–4
- [17] da Rocha-Azevedo B, Ho C H and Grinnell F 2013 Fibroblast cluster formation on 3D collagen matrices requires cell contraction dependent fibronectin matrix organization *Exp. Cell Res.* **319** 546–55
- [18] Furukawa K, Ushida T, Sakai Y, Kunii K, Suzuki M, Tanaka J and Tateishi T 2001 Tissue-engineered skin using aggregates of normal human skin fibroblasts and biodegradable material *J. Artif. Organs* **4** 353–6